ARR No. 4A22



NATIONAL ADVISORY COMMITTEE FOR AERONAUTICS

# WARTIME REPORT

ORIGINALLY ISSUED

January 1944 as
Advance Restricted Report 4A22

## EFFECTS OF HEAT-CAPACITY LAG IN GAS DYNAMICS

By Arthur Kantrowitz

Langley Memorial Aeronautical Laboratory
Langley Field, Va.



WASHINGTON

NATIONAL ADVISORY COMMITTEE FOR AERONAUTICS

ADVANCE RESTRICTED REPORT

# EFFECTS OF HEAT-CAPACITY LAG IN GAS DYNAMICS

By Arthur Kantrowitz



## SUMMARY

The existence of energy dissipations in gas dynamics, which must be attributed to a lag in the vibrational heat capacity of the gas, has been established both theoretically and experimentally.

The flow about a very small impact tube is discussed. It is shown that total-head defects due to heat-capacity lag during and after the compression of the gas at the nose of an impact tube are to be anticipated. Experiments quantitatively verifying these anticipations in carbon dioxide are discussed. A general theory of the dissipations in a more general flow problem is developed and applied to some special cases. It is pointed out that energy dissipations due to this effect are to be anticipated in turbines. Dissipations of this kind might also introduce errors in cases in which the flow of one gas is used in an attempt to simulate the flow of another gas. Unfortunately, the relaxation times of most of the gases of engineering importance have not been studied.

A new method of measuring the relaxation time of gases is introduced in which the total-head defects observed with a specially shaped impact tube are compared with theoretical considerations. A parameter is thus evaluated in which the only unknown quantity is the relaxation time of the gas. This method has been applied to carbon dioxide and has given consistent results for two impact tubes at a variety of gas velocities.

## INTRODUCTION

The heat content of gases is primarily three forms of molecular mechanical energy. First, there is the translational kinetic energy which is $\frac{3}{2}RT$, where R

is the gas constant and T is the absolute temperature. Secondly, there is the rotational kinetic energy. For all gases near or above room temperature, the n rotational degrees of freedom involving moments of inertia due to the separation of atomic nuclei have energy states close enough together that the rotational internal energy is close to the classical value $\frac{n}{2}RT$. The third principal form of internal energy is the vibrational energy of the molecules. If the frequencies of the normal modes of vibration of the molecule are known (say, from spectra), the vibrational heat capacity can be computed by the methods of statistical mechanics. (See, for example, reference 1.)

The possibility of dispersion and absorption of sound due to parts of the heat capacity lagging behind the rapid temperature changes accompanying the propagation of a sound wave in a gas was first discussed theoretically by Jeans and Einstein. Dispersion and absorption in carbon dioxide observed by Pierce were shown by Herzfeld and Rice to be attributable to lagging of the vibrational heat capacity of the gas. Kneser was able to account quantitatively for dispersion and absorption in $CO_2$ and oxygen on the assumption that the vibrational heat capacity lagged.

The dispersion and absorption of sound in several gases have been investigated and a fairly complete bibliography is available in reference 2. It is found, in general, that dispersion and absorption many times larger than those attributable to vicosity and heat conduction are to be expected in gases with vibrational heat capacity. These effects can be described by relations such as those given by Kneser and can be attributed to the vibrational heat capacity of the gas.

All the measurements of dispersion and absorption have demonstrated that most impurities markedly reduce the relaxation time of a gas; for example, Kneser and Knudsen (references 3 and 4) concluded that the adjustment of the vibrational heat capacity of oxygen was dependent entirely on the action of impurities. Various experiments with $CO_2$ have shown that, at room temperature, collisions with water molecules are 500 times as effective as collisions with $CO_2$-molecules in exciting vibration in $CO_2$-molecules. This strong

dependence on purity has produced great discrepancies among the relaxation times measured by the various workers in this field. There has been much better agreement among the measurements of the effectiveness of impurities. Sonic measurements in $CO_2$ are discussed in appendix A. A quantum-mechanical theory of relaxation times developed by Landau and Teller is discussed in appendix B. Two conclusions, which are verified by the sonic work in $CO_2$, are important to the present paper: (1) All the vibrational states of a single normal mode adjust with the same relaxation time and (2) the logarithm of the relaxation time (expressed in molecular collisions) is proportional to $T^{-\frac{1}{3}}$. Verification of conclusion (2) is presented in figure 1.

Dr. Vannevar Bush helped to initiate this work by asking the writer a stimulating question. The author also is very grateful to Professor E. Teller for helpful discussions.

## EFFECTS IN GAS DYNAMICS

In the flow of gases about obstacles, compressions and rarefactions accompanied by temperature changes occur. The time in which these temperature changes take place is controlled by the dimensions of the obstacles and the velocity of flow. If these time intervals are comparable with or shorter than the time required for the gas to absorb its full heat capacity, the gas will depart from its equilibrium partition of energy. In this case, the transfer of energy from parts of the heat capacity that have more than their share to parts that have less than their share will be an irreversible process and will increase the entropy of the gas. If the time intervals involved are comparable with the relaxation time of the gas, this increase in entropy can be used to measure the relaxation time of the gas (reference 5).

Turbine-working fluids such as steam, air, and exhaust gas have appreciable vibrational heat capacity at high temperatures. If these gases have relaxation times comparable with or shorter than the intervals during which temperature changes occur in the gas, losses

attributable to heat-capacity lag must be anticipated. A rough estimate has indicated that, unless the relaxation times of the working fluids are very short, the losses at high temperatures due to heat-capacity lag can be comparable with the losses due to skin friction. Unfortunately, no measurements of the relaxation times of the usual turbine-working fluids exist.

Various persons have proposed, in wind-tunnel tests and in tests of rotating machinery, the substitution of gases that have properties enabling tests to be made more conveniently at a given Mach number or Reynolds number than with the actual working fluid. In such cases, care must be taken to ensure that an error due to differences in heat-capacity-lag behavior of the fluid used and the working fluid is not introduced. For example, according to a rough calculation, a wing in pure $CO_2$ might have a drag coefficient twice as large as the same wing in air at the same Mach number and Reynolds number.

In the following discussion, the existence of these dissipations in gas dynamics is demonstrated and a gas-dynamics method of measuring the relaxation times is developed. The application of this method to the measurement of the relaxation times of gases of engineering importance is proposed.

## FLOW ABOUT A VERY SMALL IMPACT TUBE

As a first example of the energy dissipations to be expected from heat-capacity lag, consider the total head measured by an impact tube in a perfect gas. For definiteness, consider the apparatus illustrated schematically in figure 2. The gas enters the chamber and settles at the pressure $p_0$ and the temperature $T_0$. It then expands to a pressure $p_1$ and a temperature $T_1$ out of the faired orifice, which is designed to give a temperature drop gradual enough that the expansion through the orifice is isentropic. The gas that flows along the axial streamline of the impact tube is then brought to rest at the nose of the tube and, during this process, its pressure rises to $p_2$ and its temperature rises to $T_2$. If this second process is slow enough to be isentropic also, the entropy and the energy of the gas that has reached equilibrium at the nose of the impact tube are equal to the

values in the chamber and hence the pressure $p_2$ equals $p_0$ and the reading on the alcohol manometer is zero.

Consider, however, the other extreme case in which the compression time - that is, the time required for the gas to undergo the greater part of its temperature rise - at the nose of the impact tube is small compared with the time required for the gas to absorb its full heat capacity. The orifice is considered large enough that, during the expansion through it, the gas maintains equilibrium. A part of the heat capacity of the gas $c_{vib}$ does not follow the rise in temperature during the compression as the gas is brought to rest at the nose of the impact tube and adjusts irreversibly after the compression is over. The resultant increase of entropy in this case means that the pressure $p_2$ is lower than $p_0$. This increase in entropy is now calculated. All temperature changes are assumed small enough that the heat capacities of the gas can be taken as constants.

At the beginning of the adjustment, the lagging part of the heat capacity $c_{vib}$ is still in equilbrium with a thermometer at the temperature $T_1$ while the translational and other degrees of freedom with heat capacities totaling $c_p'$, the relaxation time of which can be neglected, are in equilibrium with a thermometer at some higher temperature T. Energy then flows from the heat capacity $c_p'$ to the heat capacity $c_{vib}$, increasing the temperature $T_{vib}$ associated with $c_{vib}$ from $T_1$ to the final equilibrium temperature, which is $T_0$. Conservation of energy gives the following relation between T and $T_{vib}$:

$$c_{vib}T_{vib} + c_p'T = c_pT_0 \qquad (1)$$

where $c_p$ is the total heat capacity at constant pressure. The entropy increase when an element of energy dq flows from T to $T_{vib}$ is

$$dS = \frac{dq}{T_{vib}} - \frac{dq}{T} = c_{vib}\, dT_{vib}\left(\frac{1}{T_{vib}} - \frac{1}{T}\right) \qquad (2)$$

Eliminating T in equation (2) from equation (1) and integrating over the whole process gives

$$\Delta S = \int_{T_1}^{T_0} c_{vib}\, dT_{vib} \left( \frac{-c_p'}{c_p T_0 - c_{vib} T_{vib}} + \frac{1}{T_{vib}} \right)$$

$$= \log \left( \frac{\frac{c_p}{c_{vib}} - 1}{\frac{c_p}{c_{vib}} - \frac{T_1}{T_0}} \right)^{c_p'} \left( \frac{T_0}{T_1} \right)^{c_{vib}} \qquad (3)$$

Equation (3) gives the entropy difference between the gas in the chamber and the gas at equilibrium at the nose of the impact tube. Because the energy and hence the temperature is the same at the beginning and at the end of the process, the ratio of chamber pressure to impact-tube pressure can readily be computed from the perfect gas relation

$$S = c_p \log T - R \log p + \text{Constant}$$

which gives

$$\Delta S = R \log \frac{p_0}{p_2}$$

and

$$\frac{p_0}{p_2} = \left( \frac{\frac{c_p}{c_{vib}} - 1}{\frac{c_p}{c_{vib}} - \frac{T_1}{T_0}} \right)^{\frac{c_p'}{R}} \left( \frac{T_0}{T_1} \right)^{\frac{c_{vib}}{R}} \qquad (4)$$

It may be instructive to derive this relation by considering the isentropic parts of the process. During the slow expansion, the enthalpy theorem (see appendix C) gives $c_p T + \frac{1}{2}u^2 = \text{Constant}$ (u is flow velocity) and, during the instantaneous compression, $c_p' T + \frac{1}{2}u^2 = \text{Constant}$,

$c_{vib}$ being omitted because it takes no part in the compression. Combining these equations gives

$$c_p(T_0 - T_1) = c_p'(T_2 - T_1) \qquad (5)$$

where $T_2$ is the temperature reached by the translational degrees of freedom before the adjustment period starts. The adiabatic-compression relation can be applied to both the expansion and the compression with the appropriate heat capacities to calculate $p_2$; thus,

$$\left(\frac{p_2}{p_1}\right)^{\frac{R}{c_p'}} = \frac{T_2}{T_1} \qquad \left(\frac{p_0}{p_1}\right)^{\frac{R}{c_p}} = \frac{T_0}{T_1} \qquad (6)$$

Combining equations (5) and (6) gives, after several manipulations,

$$\frac{p_0}{p_2} = \left(\frac{c_p - c_{vib}}{c_p - c_{vib}\frac{T_1}{T_0}}\right)^{\frac{c_p'}{R}} \left(\frac{T_0}{T_1}\right)^{\frac{c_{vib}}{R}}$$

which is of course identical with equation (4).

The percentage total-head defect $100\frac{p_0 - p_2}{p_0 - p_1}$ is plotted against chamber pressure $p_0/p_1$ in figure 3 for $c_p' = 3.5R$. The apparatus schematized in figure 2 was used to check equation (4) for $CO_2$ where the vibrational heat capacity would be expected to lag. The orifice was a hole in a $\frac{1}{2}$-inch plate with its diameter variation designed for constant time rate of temperature drop. The last 1/16 inch of the flow passage was straight in order that the streamlines in the jet would be straight and axial and hence the static pressure at the orifice exit would equal atmospheric pressure. The glass impact tube was 0.005 inch in diameter and its end

were between 300 and 600 feet per second. The expansion therefore took place in times ranging between $1.4 \times 10^{-4}$ and $2.8 \times 10^{-4}$ second. The compression at the nose of an impact tube takes place while the gas flows a distance of the order of 1 tube radius. (See fig. 5.) The compression times then ranged between $7 \times 10^{-7}$ and $14 \times 10^{-7}$ second. Commercial $CO_2$ was used and, because it was fairly dry, a relaxation time of the order of $10^{-5}$ second was expected. It seemed likely, therefore, that this setup would approach the case of an isentropic expansion and an instantaneous compression closely enough for the results to bear at least a qualitative resemblance to equation (4).

Preliminary to the investigation of heat-capacity lags, it was necessary to make sure that hydrodynamic effects other than heat-capacity lag would not produce a reading on the alcohol manometer. Air and later nitrogen at room temperature were therefore substituted for $CO_2$ at the beginning of each run. It was always found in these preliminary tests that, when the tube was properly alined, the difference in pressure measured by the alcohol manometer was very small and could be accounted for entirely by lags in the small vibrational heat capacity of air (about 0.02R).

Carbon dioxide was then introduced into the apparatus and the observations shown in figure 4 were made. The gas was heated before entering the chamber, and its temperature was measured by a small thermocouple inserted in the jet close to the impact tube. In accordance with aerodynamic experience, the temperature measured by the thermocouple was assumed to be $0.9T_0 + 0.1T_1$. The difference between $T_0$ and $T_1$ was always less than 30° F, corresponding to a difference in $c_{vib}$ of less than 8 percent, and was thus considered accurate enough to assume a constant $c_{vib}$ and to compute this value at a temperature $\overline{T} \equiv \frac{T_0 + T_1}{2}$.

The pressure $p_0 - p_1$ was read by the mercury manometer, $p_1$ by a barometer, and $p_0 - p_2$ by the

alcohol manometer, which was fitted with a microscope to make possible readings to 0.001 inch.

In figure 4 the reading of the alcohol manometer is plotted against the chamber pressure $p_0/p_1$. The experimental values at both temperatures agree with the theoretical values more closely than could have been anticipated. It will become clear later that the theoretical and experimental values agreed so closely because small entropy increases in the orifice, attributable to too-rapid expansion, just about compensated for the fact that the compression was not quite instantaneous compared with the relaxation time of the gas. It should be pointed out that ordinary hydrodynamic effects such as misalinement of the impact tube would be expected to produce a total-head defect which would vary directly as

$$\frac{p_0}{p_1} - 1 .$$

## GENERAL THEORY OF ENERGY DISSIPATIONS IN GASES EXHIBITING HEAT-CAPACITY LAG

In the general case in which the temperature changes may be neither very fast nor very slow compared with the relaxation time of the gas, the temperature history of a gas particle as it flows along a streamline must be considered. The problem is greatly simplified if the effect of heat-capacity lag on velocity distribution is neglected in order to get the effect of the lag on energy dissipation. This procedure can be regarded as the first step in an iteration process and is probably adequate for the applications now contemplated. The restriction that the temperature changes involved in the flow are small enough for the heat capacities to be considered constant is also retained.

Assume, therefore, that the velocity distribution in the field of flow is determined by standard gas-dynamics methods. The velocity distribution is usually given as a function of space coordinates $u(x,y,z)$ or along the $\sigma$-streamline as $u_\sigma(s)$, where $s$ is the distance along the streamline. This expression can be converted to a function of time $u_\sigma(t)$ by integration of $dt = \frac{ds}{u(s)}$

along a streamline. The function $u_o(t)$ is taken for granted and the entropy increase in the flow along a streamline is determined.

By introducing the variable $\epsilon$, which represents the excess energy per unit mass in the lagging heat capacity over the energy at equilibrium partition at the translational temperature $T$, it is seen that

$$c_p T + \frac{1}{2} u^2 + \epsilon = \text{Constant} \tag{7}$$

The assumption is now introduced that there is only one type of heat energy in the gas $E_{vib}$ which lags appreciably behind the translation temperature and that its time rate of adjustment is proportional to its departure from equilibrium; that is,

$$\frac{dE_{vib}}{dt} = -k\epsilon$$

This assumption is in agreement with the sonic theories previously discussed. From the definition of $\epsilon$,

$$\epsilon = E_{vib} - c_{vib} T$$

because $c_{vib} T_{vib}$ is the equilibrium value of $E_{vib}$ (measured from an arbitrary zero). By combining these equations, $E_{vib}$ can be eliminated to yield

$$\frac{d\epsilon}{dt} = -c_{vib} \frac{dT}{dt} - k\epsilon \tag{8}$$

The meaning of $k$ can be made clear if the variation of $\epsilon$ with time is examined for the case in which the total heat energy of the gas remains constant. In this case,

$$c_p T + \epsilon = \text{Constant}$$

Equation (8) then becomes

$$\frac{d\epsilon}{dt} = \frac{c_{vib}}{c_p}\frac{d\epsilon}{dt} - k\epsilon$$

or

$$\frac{d\epsilon}{dt} = -k\frac{c_p}{c_p'}\epsilon$$

from which $k\frac{c_p}{c_p'}$ is the reciprocal of the relaxation time $\tau$ of the gas. It will be seen that these equations are restricted to gases with only one relaxation time.

In order to simplify later expressions and to clarify their physical meaning, there are introduced the dimensionless variables

$$\left.\begin{aligned} \epsilon' &= \frac{\epsilon}{\frac{c_{vib}}{c_p'}\frac{U^2}{2}} & t' &= \frac{t}{h/U} \\ u' &= \frac{u}{U} & K &= \frac{h}{\tau U} \end{aligned}\right\} \qquad (9)$$

where $h$ and $U$ are a typical length and a typical velocity in the flow and $K$ is a dimensionless parameter that is a measure of the ratio of the times in which temperature changes occur in the gas to the relaxation time of the gas. It will be seen later that $\epsilon'$ is defined to make it become unity after an instantaneous expansion which starts from rest with equilibrium energy partition and ends with the velocity $U$. Eliminating $T$ between equations (7) and (8) and introducing the nondimensional quantities gives

$$\frac{d\epsilon'}{dt'} + K\epsilon' = \frac{du'^2}{dt'} \qquad (10)$$

If $u'(t')$ is known, the integral of equation (10) can be written as

$$\epsilon' = e^{-\int K dt'} \left( \int \frac{du'^2}{dt'} e^{\int K dt'} \, dt' + \text{Constant} \right) \tag{11}$$

The rate of entropy increase in the flow can now be calculated from equation (11). The rate of heat flow from the temperature $T_{vib}$ to $T$ is $k\epsilon$; hence,

$$\frac{dQ}{dt} = k\epsilon \left( \frac{1}{T} - \frac{1}{T_{vib}} \right) \tag{12}$$

Now $\epsilon = c_{vib} \left( T_{vib} - T \right)$ and equation (12) can be written as

$$\frac{dQ}{dt} = k\epsilon \left( \frac{1}{T} - \frac{1}{T + \frac{\epsilon}{c_{vib}}} \right)$$

The entropy increase along the streamline in question between the starting time $t_0$ and the time $t$ is

$$\Delta S = \int_{t_0}^{t} k\epsilon \left( \frac{1}{T} - \frac{1}{T + \frac{\epsilon}{c_{vib}}} \right) dt \tag{13}$$

In order to obtain the total entropy increase, equation (13) would have to be integrated over all the streamlines in the flow with the use of equation (7).

## Similarity Law for Low-Velocity Flows

The calculation of energy dissipations can be simplified if the restriction to flows involving pressure and temperature changes that are small compared with ambient pressure and temperature is adopted. The greatest advantage of this procedure is that the flow pattern obtained in an incompressible fluid can be used as an approximation. This fact is important because few compressible fluid flows are known accurately. If this restriction is accepted, $k$ and hence $K$ can be assumed constant for the flow. Equation (11) then becomes

$$\epsilon' = e^{-Kt'} \left( \int \frac{du'^2}{dt'} e^{Kt'} \, dt' + \text{Constant} \right) \tag{14}$$

Now both $\frac{\epsilon}{c_{vib}}$ and variations of $T$ are small compared with $T$ and equation (13) becomes

$$\Delta S = \frac{k}{c_{vib}\bar{T}^2} \int_{t_0}^{t} \epsilon^2 \, dt \qquad (15)$$

It is now shown that there is a simple relation among the dependencies of the energy dissipation in a low-velocity flow on the scale of the flow, on the typical velocity, and on the relaxation time of the gas. This relation is that the entropy increase, reduced to nondimensional form, depends in geometrically similar flows on a single parameter $K$.

Equation (15) can be rewritten as

$$\Delta S = \frac{c_p' K}{c_p c_{vib} \bar{T}^2} \left( \frac{U^2}{2} \frac{c_{vib}}{c_p'} \right)^2 \int_{t'_0}^{t'} \epsilon'^2 \, dt'$$

Introducing the nondimensional entropy increase $\Delta S'$ by dividing $\Delta S$ by the entropy increase following an "instantaneous" compression gives

$$\Delta S' = 2K \int_{t'_0}^{t'} \epsilon'^2 \, dt' \qquad (16)$$

From equation (14), it is known that $\epsilon'$ and hence $\Delta S'$ depends only on $K$ for similar flows.

## Approximations for Large and Small Values of $K$

The integrations of equations (14) and (16) are sometimes difficult to perform analytically and laborious to evaluate numerically. For the special cases in which the relaxation time is either long or short compared with the times in which temperature changes take place in the gas, it is possible to use approximations that considerably reduce the numerical labor. In these cases, it is possible to express $\Delta S'$ in terms of integrals in which

K does not appear under the integral sign; thus, these integrals need be evaluated only once to determine $\Delta S'$ for all values of K for which the approximation is valid.

The case of short relaxation time, when K is large, will be treated first. In order to avoid confusion, the symbol $t'_a$ is introduced into equation (14), which becomes

$$\epsilon'(t'_a) = \int_{t'_0}^{t'_a} \frac{du'^2}{dt'} e^{-K(t'_a - t')}\, dt' \qquad (17)$$

For a large value of K, most of the contribution to this integral comes from values of $t'$ so close to $t'_a$ that the following approximations can be made:

$$\frac{du'^2}{dt'} = \left(\frac{du'^2}{dt'}\right)_a \qquad t' - t'_a \doteq \frac{u'^2 - u'^2_a}{\left(\frac{du'^2}{dt'}\right)_a}$$

and the lower limit of the integral in equation (17) can be replaced by $\pm\infty$. Equation (17) then becomes

$$\epsilon'(t'_a) = \int_{\pm\infty}^{u'^2_a} \exp\left[\frac{K}{\left(\frac{du'^2}{dt'}\right)_a}(u'^2 - u'^2_a)\right] du'^2$$

where the sign of the lower limit is opposite that of $\left(\frac{du'^2}{dt'}\right)_a$. Hence, for $K \gg 1$,

$$\epsilon'(t'_a) = \frac{1}{K}\left(\frac{du'^2}{dt'}\right)_a \qquad \Delta S' = \frac{2}{K}\int \left(\frac{du'^2}{dt'}\right)^2 dt' \qquad (18)$$

The case of long relaxation time, when K is small compared with 1, is now considered. In the usual flow problem, the gas velocity changes appreciably during a certain time interval - say, from 0 to $t'_1$ - and then

settles to a new steady value. The problem can be divided into two parts: $0 < t' < t'_1$ and $t' > t'_1$. If $K$ is small enough, the change in $\epsilon'$ due to the $\epsilon'$-term in equation (10) is small compared with the change due to the $\frac{du'^2}{dt'}$-term and can be neglected in the calculation of the entropy increase $\Delta S'_1$ during the first interval; thus,

$$\epsilon' = u'^2 - u'_0{}^2$$

where $u'_0{}^2$ is the velocity squared at $t' = 0$. Hence,

$$\Delta S'_1 = 2K \int_0^{t'_1} \epsilon'^2 \, dt' = 2K \int_0^{t'_1} \left(u'^2 - u'_0{}^2\right)^2 dt'$$

In order to compute the value of $\epsilon'$ at $t'_1$, the total contribution of the $\epsilon'$-term in equation (10) is added to the total change in the square of the velocity during the first interval $\Delta u'^2$. Thus,

$$\epsilon'_1 = \Delta u'^2 - K \int_0^{t'_1} \epsilon' \, dt' = \Delta u'^2 - K \int_0^{t'_1} \left(u'^2 - u'_0{}^2\right) dt'$$

In the period after $t'_1$,

$$\epsilon' = \epsilon'_1 e^{-K(t'-t'_1)}$$

and the entrcpy increase in this second period $\Delta S'_2$ is

$$\Delta S'_2 = 2K\epsilon'_1{}^2 \int_{t'_1}^{\infty} e^{-2K(t'-t'_1)} \, dt' = \epsilon'_1{}^2$$

The total entropy increase in the flow is therefore, for $K \ll 1$,

$$\Delta S' = 2K \int_0^{t'_1} \left(u'_0{}^2 - u'^2\right)^2 dt'$$

$$+ \left[ K \int_0^{t'_1} \left(u'_0{}^2 - u'^2\right) dt' + \Delta u'^2 \right]^2$$

## Calculation of Total-Head Defect in Flow about a "Source-Shaped" Impact Tube

The total-head defect to be anticipated in a compression at the nose of an impact tube of a special shape is calculated to be used in the measurement of the relaxation time of gases. The restriction to low velocities adopted previously is retained, chiefly to permit the use of incompressible-fluid theory and of the similarity theorem.

The flow about bodies of revolution in a uniform stream is usually calculated by considering the flow about sources in the fluid. (Compare reference 6, p. 146.) It is possible to find a surface in the flow across which no fluid flows. If a solid body shaped like this surface is substituted for the sources, no alteration outside the surface occurs; the flow about the solid body is thus identical with that about the sources. The flow about a single source in a uniform flow is calculated in reference 6 and the corresponding shape is plotted in figure 5. The total-head defect to be anticipated for a tube of this shape is calculated as follows:

The velocity along the central streamline is required. This velocity is given on page 147 of reference 6 and is plotted in figure 5 as

$$u(x) = U\left(1 - \frac{d^2}{16x^2}\right)$$

where

$x$ distance along central streamline from source

$U$ velocity far from body

$d$ diameter of impact tube

This expression can be converted to the following non-dimensional form by using $U$ as the typical velocity and $d$ as the typical dimension:

$$u'(x') = 1 - \frac{1}{16x'^2} \tag{19}$$

The next step is to find $u'(t')$. The quantity $t'$ can be found as a function of $u'$ by integrating

$$dt' = \frac{dx'}{u'(x')} = -\frac{1}{8}\frac{du'}{u'(1 - u')^{3/2}}$$

The choice of the zero of $t'$ is arbitrary. For convenience, if $t' = 0$ when $u' = 0.99$, then

$$t' = -\frac{1}{8}\int_{0.99}^{u'} \frac{du'}{u'(1 - u')^{3/2}}$$

$$= -\frac{1}{8}\left[\log\left(\frac{11}{9}\frac{1 - \sqrt{1 - u'}}{1 + \sqrt{1 - u'}}\right) + \frac{2}{\sqrt{1 - u'}} - 20\right] \tag{20}$$

The next step is to determine $\epsilon'(t')$ from equation (14). Then, by use of equation (19),

$$\frac{du'^2}{dt'} = 2u'^2\frac{du'}{dx'} = -16u'^2(1 - u')^{3/2} \tag{21}$$

Because $\epsilon'$ is zero initially ($t' = -\infty$) and remains zero until $u'$ begins to vary rapidly with time, if $K$ is not

too small, the lagging heat capacity can be assumed to follow the temperature changes in the gas up to the point $u' = 0.99$; that is, $\epsilon' = 0$ can be used for $t' = 0$. Combining this fact with equations (14) and (21) yields

$$\epsilon'(t') = -e^{-Kt'} \int_0^{t'} 16u'^2(1 - u')^{3/2} e^{Kt'} \, dt' \qquad (22)$$

In view of the partly transcendental nature of equation (20), it was necessary to integrate equation (22) numerically. Equation (20) was plotted (fig. 6) in such a way that the values of $u'$ corresponding to regularly spaced values of $t'$ could be found easily. By Simpson's rule, $\epsilon'(t')$ was then found for a series of values of $K$. An example of the result of such a calculation is given in figure 6 for $K = 3$. The entropy increase along the central streamline was then found from equation (16).

Values of $\Delta S'$ found from integrating equation (22) by Simpson's rule and equation (16) with a planimeter are plotted in figure 7 and are given in the following table:

RESULTS OF NUMERICAL CALCULATIONS OF $\Delta S'$

FOR SOURCE-SHAPED IMPACT TUBE

| K | $\Delta S'$ |
|---|---|
| 10 | 0.1685 |
| 3 | .405 |
| 2 | .516 |
| 1 | .676 |
| .3 | .868 |
| .1 | .952 |

For large and small values of $K$, the approximations developed earlier were used to reduce the labor of calculations and yielded the result $\Delta S' = 1.743/K$ when $K$ is large and $\Delta S' = 1.452K + (1 - 1.008K)^2$ when $K$ is small. These results are plotted in figure 7; this figure thus indicates the range of applicability of these approximations.

## Calculation of Entropy Increase in Flow through a Nozzle of Special Design

For the measurements of the relaxation time in $CO_2$, a nozzle is employed in which the gases expand and accelerate before meeting the impact tube. This expansion cannot always be made slow enough - that is, the nozzle large enough - that the expansion through the nozzle involves a really negligible entropy increase; hence, the results of figure 7 must be corrected for the entropy increases in the nozzle. In order to simplify the calculations, the nozzle was so designed that the time rate of temperature drop was constant. It can be shown that the entropy increase in a nozzle of this design is

$$\Delta S' = \frac{4}{3K_N} - \frac{16}{9K_N^2}\left(1 - e^{-\frac{3}{2}K_N}\right) + \frac{4}{9K_N^2}\left(1 - e^{-3K_N}\right)$$

where $K_N = \frac{l}{U_T}$ and $U$ is the final velocity attained by the flow in the nozzle. It must be remembered that the calculations for the impact tube presumed $\epsilon'$ to be zero initially. This condition is the case only if $K_N \gg 1$ and hence the calculation given here is valid only for this case.

From the definitions of $K$ and $K_N$, it is seen that $K_N = \frac{l}{d}K$ and hence the total entropy increase

$$\Delta S'_T = \Delta S'_{tube} + \Delta S'_N$$

can be expressed as a function of $K$ alone for a given $l/d$. This total entropy increase is plotted in figure 8 against $K$ for the two values of $l/d$ used in these experiments and for $l/d = \infty$.

## MEASUREMENT OF RELAXATION TIME OF $CO_2$

The theory will now be applied to the measurement of the relaxation time of $CO_2$. This work was undertaken both to test the theory and to develop a

technique that would supplement the sonic methods previously used for measuring relaxation times. The method essentially consists in expanding the gas through a known pressure ratio in a nozzle and compressing it again at the nose of a source-shaped impact tube. The resultant total-head loss is divided by the total-head loss that would be obtained in a very slow expansion and a fast compression (equation (4)). This nondimensional total-head loss is compared with a theoretical result such as is shown in figure 8 and the value of K appropriate to the flow is found. From this value of K, the relaxation time of the gas can be easily computed if the velocity before compression and the diameter of the impact tube are know.

During the compression of the gas, the temperature and pressure rise from $T_1$ and $p_1$ to $T_2$ and $p_2$, respectively. The relaxation time and the heat capacity of the gas thus change along a streamline. The procedure previously outlined then gives an average relaxation time for the flow. It is assumed that this average relaxation time is the relaxation time appropriate to conditions halfway between compressed and expanded conditions. Because $p_2$ is close to $p_0$ and $T_2 = T_0$, these conditions $\overline{p}$ and $\overline{T}$ can be found from

$$\overline{p} = \frac{p_0 + p_1}{2}$$

and

$$\overline{T} = \frac{T_0 + T_1}{2}$$

The errors introduced in this way certainly are no greater than those due to the low-velocity assumption introduced in the theory upon which figure 8 is based.

## Gas

The gas used in these experiments was commercial "bone-dry" $CO_2$. This gas was dried by passing it through calcium chloride and then dehydrite while it

was at a pressure greater than 40 atmospheres. The purification procedure was not so thorough as methods used in some previous investigations, and it is to be expected that somewhat shorter relaxation times would be obtained. The primary object of this work is to establish the self-consistency of this test method rather than to obtain an accurate relaxation time for pure $CO_2$.

## Apparatus

The apparatus used is essentially the same as that schematized in figure 2. A longitudinal section through a chamber of the most recent design is shown in figure 9. (The chamber used in the tests discussed in the next section did not incorporate the liner and the gas entered from the bottom.) The gas enters through three holes that were made small to stabilize the gas flow into the chamber. The glass wool is necessary to remove turbulence from the gas in the chamber and contributes materially toward reducing the total-head defects obtained in gases without heat-capacity lag. It was found that total-head defects traceable to nonuniformities in temperature existed and could be reduced by the use of the lined chamber shown. The fact that the gas flows around the inner chamber before entering helps to keep the gas in the inner chamber at uniform temperature.

The temperature nonuniformities can be almost eliminated if the gas entering the outer chamber is at the same temperature as the chamber. A mechanism was used to adjust the alinement of the impact tube without moving the tip from the center of the nozzle. The impact tube must be adjustable in order that small errors in shape near the hole will not give spurious total-head defects (in helium, for example). The gas and the chamber were heated electrically and a thermocouple inside the chamber was used to measure the gas temperature.

The nozzle used had a circular cross section, was 1.6 inches long, and was designed according to the methods previously described to give a constant time rate of temperature drop; that is, $\frac{du^2}{dt} = \text{Constant}$ for the first 1.5 inches, the last 0.1 inch being straight. The radius of the nozzle $r$ is plotted against the distance along the center line $x$ in figure 10.

Two impact tubes with diameters 0.0299 inch and 0.0177 inch were used in these experiments. They were made by drawing out glass tubing until a piece of appropriate diameter and hole was obtained. The hole was kept larger than about 0.004 inch and the fine section not too long (≈1/4 in.) to prevent the response of the alcohol manometer from being too sluggish. The ends of the tubes were ground to a source shape (fig. 5) on a fine stone. During the grinding process, a silhouette of the tube was cast on the screen of a projecting microscope and the contour superimposed on a source-shaped curve. By this technique the contour could be ground to the source shape within 0.0005 inch, except for the hole, in a short time.

## Tests and Computations

The total-head defect in $CO_2$ was measured with the two impact tubes over a range of chamber pressures. The consistency of relaxation times obtained at various pressure ratios and with various impact tubes serves as a check on this method of measuring relaxation time and on the theory on which the method is based.

Before each series of measurements nitrogen, which has only a negligible vibrational heat content at room temperature, was run through the chamber to be sure that no spurious effects and leaks were present. In the results reported herein, the errors due to these effects were kept to less than 0.01 percent of the chamber pressure; therefore, the resultant error in relaxation time due to these causes was less than 4 percent. In subsequent work (not reported herein), it was found that most of these total-head aberrations could be eliminated by ensuring uniform temperature in the issuing gases. If care is taken to eliminate temperature nonuniformities, tube misalinements, and turbulence in the chamber, the total-head aberrations can be reduced to 0.002 percent or less.

The total-head defects obtained were divided by the result of equation (4) to reduce them to nondimensional form. The appropriate value of $K$ was found by referring to the appropriate curve in figure 8. The gas velocity was computed from the reading of the mercury manometer by the enthalpy theorem with adiabatic expansion

assumed. The relaxation time was then computed from the definition of $K$ by equation (9). The relaxation times thus obtained were expressed in collisions per molecule. The number of molecular collisions per second in $CO_2$ was assumed to be $8.888 \times 10^9$ at 15° C and 1 atmosphere by combining tables of pages 26 and 149 of reference 7. At all other temperatures and pressures, the number of collisions was assumed to vary inversely with $\sqrt{T}$ and directly with pressure. The number of molecular collisions per second and the heat capacity of the gas were computed at temperature $\overline{T}$ and pressure $\overline{p}$. The data obtained are given in tables I and II for the 0.0299- and 0.0177-inch tubes, respectively.

The results are plotted in figure 11, which indicates that the relaxation time in collisions is nearly independent of pressure ratio and impact-tube size. This consistency constitutes the desired verification of this test method. It was expected that a variation at high pressure ratios would appear in view of the assumption of low velocity made at several points in the theoretical development.

A large part of the scatter of the results in figure 11, in particular the apparent drop at low pressures, is attributed to the fact that in the tests the average temperature (halfway between chamber and expanded temperatures) was not held constant during the run.

The average number of collisions obtained with the 0.0299-inch tube was 33,100; with the 0.0177-inch tube, 32,000. The final result at 105° F thus is 32,600, which is somewhat lower than the result of recent investigations in which the $CO_2$ has been much more carefully purified than in the present investigation. (Compare with fig. 1.)

## IMPACT-TUBE METHOD OF MEASURING RELAXATION TIME OF GASES

The impact-tube method of measuring the relaxation time of gases rests essentially on the fact that the total-head defect not traceable to heat-capacity lag can be reduced to a very small value - say, 0.002 percent. Very small dissipations due to heat-capacity lag are therefore measurable. For example, a gas having a

lagging heat capacity 0.1R with a relaxation time of $10^{-7}$ second could give a total-head defect of 0.05 percent. If the gas had a lagging heat capacity as large as R, a relaxation time as short as $10^{-8}$ second would be measurable.

This method seems to be easier to carry out than the sonic methods previously discussed and can be used to measure relaxation times with comparable precision. The quantity of gas required to make a measurement will be larger than for the sonic methods (a standard tank of $CO_2$ lasts about 5 hr in this apparatus) and thus may make it more difficult to attain high purity.

If the gas to be studied has a long relaxation time - greater than 50 microseconds, for example - it should be possible to measure the relaxation time in an apparatus similar to the one discussed by comparing the total-head defects obtained with a calculation of the entropy increase in the nozzle. In this case, the time taken for the gas to flow through the nozzle is compared with the relaxation time of the gas. The shape of the impact tube would be unimportant in this case as long as it was small enough that $K \ll 1$.

## CONCLUSIONS

The existence of energy dissipations in gas dynamics, which must be attributed to a lag in the vibrational heat capacity of the gas, has been established both theoretically and experimentally.

An approximate method of calculating the entropy increase in a general flow problem has been developed. The special case in which a gas at rest expands out of a specially shaped nozzle and is compressed at the nose of a source-shaped impact tube near the mouth of the nozzle has been treated, and the dependence of the resultant total-head defect on the relaxation time of the gas has been found.

The total-head defect in this flow has been applied to measure the relaxation time of $CO_2$. The results obtained with two impact tubes were in agreement within

about 3 percent. The consistency of these results is regarded as a check on the general theory developed and on this measurement method.

Langley Memorial Aeronautical Laboratory,
National Advisory Committee for Aeronautics,
Langley Field, Va.

# APPENDIX A

## SONIC MEASUREMENTS IN CARBON DIOXIDE

Much careful work has been done on the lag in the vibrational heat capacity of $CO_2$. Carbon dioxide is a linear molecule and thus has a translational and rotational heat capacity of $\frac{5}{2}R$. It has four normal modes in vibration that are diagrammed with their frequencies as follows (data from reference 8):

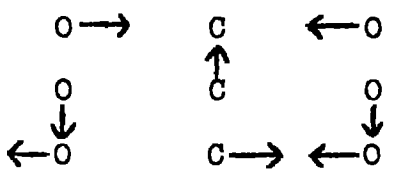

$\nu_1 = 4.164 \times 10^{13}$

$\nu_2 = 2.003 \times 10^{13}$ (2 modes)

$\nu_3 = 7.050 \times 10^{13}$

The heat capacity of $CO_2$ is somewhat complicated by the fact that the second excited state of the oscillation $\nu_2$ has almost the same energy as the first excited state of $\nu_1$. The near resonance results in a strong interaction through the first-order perturbation (the first-order departure of the potential energy from the square law) between the two states involved, as was pointed out by Fermi (reference 9). This perturbation produces significant disturbances ($\approx 50$ cm$^{-1}$) of the levels involved but does not have a large effect on the heat capacity of the gas. The heat capacity of $CO_2$ was computed by Kassel (reference 10) and his results are used in the present calculations.

Eucken and his coworkers have carefully studied over a period of years the dispersion of sound in $CO_2$ (references 11 to 15). One conclusion of this work - that the vibrational energy levels in $CO_2$ adjust with the same relaxation time - is demonstrated by showing that the dispersion curves obtained fit a simple dispersion formula such as Kneser's.

Küchler, for example, obtained a simple dispersion curve at 410° C, at which appreciable heat capacity due to all three normal modes would be expected. Richards and Reid (reference 16) and others (see bibliography of

reference 2) have maintained that the symmetrical valence vibration $\upsilon_1$ of $CO_2$ does not adjust at 9 kilocycles in some dispersion measurements made near room temperature. As they point out, this fact is remarkable because the second excited state of $\upsilon_2$ strongly perturbs the first excited state of $\upsilon_1$. In any case, the contribution of this normal mode to the heat capacity is very small at room temperature and the effects found are near the limits of the accuracy of Richards and Reid.

The relaxation time of $CO_2$ in molecular collisions, as given by Eucken and his coworkers, is plotted against $T^{-\frac{1}{3}}$ (T in °K) in figure 1 for comparison with the theory discussed in appendix B. Van Itterbeek, de Bruyn, and Mariëns (reference 17) measured the absorption at 599 kilocycles in very carefully purified $CO_2$. Their measurements, which are also given in figure 1, show a longer relaxation time than the measurements of Eucken and his coworkers. They attribute this increased relaxation time to careful purification of the gas.

All the measurements with $CO_2$ have indicated that the relaxation time is inversely proportional to the pressure of the gas. This result shows that the process responsible for the interchange of energy between vibrational and other degrees of freedom is bimolecular.

## APPENDIX B

## THEORY OF EXCITATION OF MOLECULAR VIBRATION BY COLLISIONS

Landau and Teller (reference 18) have given an approximate calculation of the probability of the excitation of a vibrational quantum in a molecular collision. Assuming that the interaction energy which induces the vibration depends linearly on the normal coordinate of a harmonic vibration, they make a first-order perturbation calculation. The matrix element for the transition from the $l$th to the $(l + 1)$th or from the $(l + 1)$th to the $l$th vibrational state is then proportional to $\sqrt{l + 1}$. The transition probabilities $k_{ij}$ are proportional to the square of matrix elements and therefore

$$k_{01}:k_{12}:k_{23} = k_{10}:k_{21}:k_{32} = 1:2:3$$

and, when $i - j \neq \pm 1$, $k_{ij} = 0$. This result is shown in reference 18 to lead to the prediction that all the allowed transitions in a given normal mode have the same relaxation time. Landau and Teller next examine the collision process classically, assuming the interaction energy between translation and vibration to be proportional to $e^{-\frac{x}{a}}$, where $x$ is the distance between the molecules and $a$ is an undetermined constant. They also assume that the translational energy of the molecules - that is, the collision - is adiabatic. The amount of energy transferred to vibration in a collision is then calculated and used to estimate the transition probability $k_{01}$ and the relaxation time of the gas. They conclude that the temperature variation of the relaxation time expressed in molecular collisions is given by

$$\text{Collisions} \propto \exp\left(3T^{-\frac{1}{3}}\sqrt[3]{\frac{(\pi a v)^2 M}{2R}}\right)$$

where $M$ is molecular weight.

In figure 1, experimental results for the relaxation time in collisions of $CO_2$ and nitrous oxide $N_2O$ are

plotted against $T^{-\frac{1}{3}}$. The theoretical results are seen to be straight lines, within experimental error. The value of $a$ can be found from the slope of the straight line. For $CO_2$ with $\upsilon = 2.003 \times 10^{13}$, $a = 0.22 \times 10^{-8}$ cm and, for $N_2O$ with $\upsilon = 1.773 \times 10^{13}$; $a = 0.36 \times 10^{-8}$ cm. These reasonable values for $a$ are a further check on this theory.

It should be pointed out that the temperature variation of catalytic effects is quite different from that of pure gases, the number of collisions required being nearly independent of temperature. (See Küchler, reference 15.) Various attempts have been made to associate the effectiveness of catalysts with their physical or chemical properties but no generally successful rule seems to have been proposed. Gases that have some chemical affinity, gases with large dipole moments, and gases with small moments of inertia are usually most effective.

## APPENDIX C

## THE ENTHALPY THEOREM

If no energy is transmitted across the walls of a stream tube, the total energy (Internal energy $E$ plus Kinetic energy per unit mass $\frac{1}{2}u^2$) plus the work done by pressures $pV$ must be the same at any cross section of the tube; that is,

$$E + \frac{1}{2}u^2 + pV = \text{Constant} \tag{C1}$$

In the case of a perfect gas with constant heat capacity and with equilibrium partition of energy, equation (C1) becomes

$$c_p T + \frac{1}{2}u^2 = \text{Constant} \tag{C2}$$

where $c_p$ is the heat capacity at constant pressure and $T$ is the absolute temperature. Whenever equilibrium partition exists, even though nonequilibrium states have been passed through, equation (C1) is applicable in the absence of viscosity and heat conduction and equation (C2) can be applied to perfect gases, provided the heat capacity of the gas can be considered constant.

## REFERENCES

1. Fowler, R. H., and Guggenheim, E. A.: Statistical Thermodynamics. The Macmillan Co., 1939.

2. Richards, William T.: Supersonic Phenomena. Rev. Modern Phys., vol. 11, no. 1, Jan. 1939, pp. 36-64.

3. Kneser, H. O.: Interpretation of Anomalous Sound-Absorption in Air and Oxygen in Terms of Molecular Collisions. Jour. Acous. Soc. Am., vol. 5, no. 2, Oct. 1933, pp. 122-126.

4. Knudsen, Vern O.: The Absorption of Sound in Air, in Oxygen, and in Nitrogen - Effects of Humidity and Temperature. Jour. Acous. Soc. Am., vol. 5, no. 2, Oct. 1933, pp. 112-121.

5. Kantrowitz, Arthur: Effects of Heat Capacity Lag in Gas Dynamics. Let. to Ed., Jour. Chem. Phys., vol. 10, no. 2, Feb. 1942, p. 145.

6. Tietjens, O. G.: Fundamentals of Hydro- and Aeromechanics. McGraw-Hill Book Co., Inc., 1934.

7. Kennard, Earle H.: Kinetic Theory of Gases. McGraw-Hill Book Co., Inc., 1938.

8. Dennison, David M.: The Vibrational Levels of Linear Symmetrical Triatomic Molecules. Phys. Rev., vol. 41, no. 3, 2d ser., Aug. 1, 1932, pp. 304-312.

9. Fermi, E.: Raman Effect in $CO_2$. Zeitschr. f. Phys., vol. 71, nos. 3 and 4, Aug. 15, 1931, pp. 250-259.

10. Kassel, L. S.: Thermodynamic Functions of Nitrous Oxide and Carbon Dioxide. Jour. Am. Chem. Soc., vol. 56, no. 9, Sept. 1934, pp. 1838-1842.

11. Eucken, A., and Becker, R.: Excitation of Intramolecular Vibrations in Gases and Gas Mixtures by Collisions, Based on Measurements of Sound Dispersion. Preliminary Communication. Zeitschr. f. phys. Chem., Abt. B, vol. 20, no. 5/6, April 1933, pp. 467-474.

12. Eucken, A., and Becker, R.: Excitation of Intramolecular Vibrations in Gases and Gas Mixtures by Collisions, Based on Measurements of Sound Dispersion. Part II. Zeitschr. f. phys. Chem., Abt. B, vol. 27, nos. 3 and 4, Dec. 1934, pp. 235-262.

13. Eucken, A., and Jaacks, H.: Excitation of Intramolecular Vibrations in Gases and Gas Mixtures by Collisions, Based on Measurements of Sound Dispersion. Part III. Zeitschr. f. phys. Chem., Abt. B, vol. 30, nos. 2 and 3, Oct. 1935, pp. 85-112.

14. Eucken, A., and Nümann, E.: Excitation of Intramolecular Vibrations in Gases and Gas Mixtures by Collisions. Part IV. Zeitschr. f. phys. Chem., Abt. B, vol. 36, no. 3, July 1937, pp. 163-183.

15. Küchler, L.: Excitation of Intramolecular Vibrations in Gases and Gas Mixtures by Collisions. Part V. Zeitschr. f. phys. Chem. Abt. B, vol. 41, no. 3, Oct. 1938, pp. 199-214.

16. Richards, W. T., and Reid, J. A.: Acoustical Studies. Part III. Rates of Excitation of Vibrational Energy in $CO_2$, $CS_2$, and $SO_2$. Jour. Chem. Phys., vol. 2, no. 4, April 1934, pp. 193-205. Part IV. Collision Efficiencies of Various Molecules in Exciting the Lower Vibrational States of Ethylene. Excitation of Rotational Energy in Hydrogen. Jour. Chem. Phys., vol. 2, no. 4, April 1934, pp. 206-214.

17. van Itterbeek, A., de Bruyn, P., and Mariëns, P.: Measurement on the Absorption of Sound in $CO_2$ Gas . . . and also in Mixtures of $CO_2$ . . . Physica, vol. 6, no. 6, June 1939, pp. 511-518.

18. Landau, L., and Teller, E.: Theory of Sound Dispersion. Phys. Zeitschr. der Sowjetunion, vol. 10, no. 1, 1936, pp. 34-43.

TABLE I.- DATA AND CALCULATIONS FOR ∅.0299-INCH TUBE

| 1 | 2 | 3 | 4 | 5 | 6 | 7 | 8 | 9 |
|---|---|---|---|---|---|---|---|---|
| Chamber pressure, $p_0/p_1$ (atm) | Total-head defect, $100\frac{\frac{p_0}{p_2} - 1}{\frac{p_0}{p_1} - 1}$ (percent) | Average temperature, $\overline{T}$ ($^\circ$F) | Total-head defect from inst. compression theory, $100\frac{\frac{p_0}{p_2} - 1}{\frac{p_0}{p_1} - 1}$ (percent) | Total $\Delta S'$ $\left(\frac{\text{Col. 2}}{\text{Col. 4}}\right)$ | K (from fig. 8) | Gas velocity at end of nozzle, U (in./sec) | Relaxation time, $\tau = \frac{d}{Uk}$ (microsec) | Collisions ($\tau \times$ Collisions per molecule per sec) |
| 1.185 | 0.321 | 115.0 | 0.611 | 0.525 | 2.03 | 5640 | 2.61 | 24,000 |
| 1.253 | .482 | 109.8 | .815 | .591 | 1.58 | 6464 | 2.93 | 27,800 |
| 1.323 | .669 | 107.5 | 1.024 | .653 | 1.23 | 7188 | 3.38 | 33,200 |
| 1.388 | .805 | 100.7 | 1.198 | .672 | 1.13 | 7731 | 3.42 | 34,700 |
| 1.464 | .966 | 101.6 | 1.412 | .684 | 1.07 | 8336 | 3.35 | 35,100 |
| 1.527 | 1.088 | 98.2 | 1.577 | .690 | 1.05 | 8761 | 3.25 | 35,000 |
| 1.580 | 1.193 | 96.1 | 1.706 | .699 | 1.01 | 9090 | 3.26 | 35,900 |
| 1.672 | 1.344 | 93.9 | 1.934 | .695 | 1.025 | 9611 | 3.04 | 34,700 |
| 1.734 | 1.445 | 92.6 | 2.076 | .696 | 1.02 | 9936 | 2.95 | 34,500 |
| 1.738 | 1.467 | 92.4 | 2.084 | .704 | .982 | 9955 | 3.06 | 35,900 |
| 1.295 | .586 | 107.8 | .941 | .623 | 1.38 | 6910 | 4.17 | 30,400 |
| 1.350 | .721 | 105.4 | 1.098 | .656 | 1.21 | 7423 | 3.33 | 33,100 |
| 1.364 | .758 | 111.5 | 1.152 | .658 | 1.21 | 7591 | 3.25 | 32,400 |
| 1.422 | .880 | 107.2 | 1.312 | .671 | 1.14 | 8051 | 3.26 | 33,300 |
| 1.499 | 1.025 | 99.2 | 1.502 | .682 | 1.075 | 8573 | 3.25 | 34,500 |
| 1.552 | 1.130 | 98.1 | 1.641 | .688 | 1.05 | 8926 | 3.19 | 34,700 |
| | | | | | | | | Av. 33,100 |

TABLE II.- DATA AND CALCULATIONS FOR 0.0177-INCH TUBE

| 1 | 2 | 3 | 4 | 5 | 6 | 7 | 8 | 9 |
|---|---|---|---|---|---|---|---|---|
| Chamber pressure, $p_0/p_1$ (atm) | Total-head defect, $100\frac{\frac{p_0}{p_2} - 1}{\frac{p_0}{p_1} - 1}$ (percent) | Average temperature, $\overline{T}$ ($^\circ$F) | Total-head defect from inst. compression theory, $100\frac{\frac{p_0}{p_2} - 1}{\frac{p_0}{p_1} - 1}$ (percent) | Total $\Delta S'$ $\left(\frac{\text{Col. 2}}{\text{Col. 4}}\right)$ | K (from fig. 8) | Gas velocity at end of nozzle, U (in./sec) | Relaxation time, $\tau = \frac{d}{Uk}$ (microsec) | Collisions ($\tau \times$ Collisions per molecule per sec) |
| 1.442 | 1.014 | 97.7 | 1.342 | 0.756 | 0.73 | 8146 | 2.98 | 31,700 |
| 1.315 | .765 | 127.3 | 1.041 | .735 | .81 | 7232 | 3.02 | 29,700 |
| 1.334 | .748 | 106.1 | 1.057 | .708 | .92 | 7289 | 2.64 | 26,700 |
| 1.389 | .900 | 98.8 | 1.196 | .753 | .74 | 7723 | 3.11 | 32,400 |
| 1.278 | .633 | 100.8 | .876 | .723 | .85 | 6687 | 3.11 | 30,800 |
| 1.229 | .519 | 110.1 | .742 | .699 | .97 | 6182 | 2.95 | 28,400 |
| 1.205 | .480 | 121.1 | .683 | .704 | .93 | 5940 | 3.20 | 30,200 |
| 1.467 | 1.100 | 103.4 | 1.429 | .770 | .67 | 8377 | 3.15 | 33,700 |
| 1.686 | 1.521 | 95.2 | 1.972 | .772 | .67 | 9703 | 2.72 | 32,000 |
| 1.612 | 1.383 | 96.0 | 1.788 | .774 | .67 | 9283 | 2.85 | 32,500 |
| 1.665 | 1.495 | 95.0 | 1.919 | .779 | .65 | 9585 | 2.84 | 33,100 |
| 1.581 | 1.317 | 95.1 | 1.708 | .771 | .67 | 9088 | 2.91 | 32,800 |
| 1.556 | 1.283 | 96.1 | 1.644 | .780 | .64 | 8937 | 3.09 | 34,500 |
| 1.548 | 1.276 | 99.2 | 1.637 | .780 | .64 | 8912 | 3.10 | 34,400 |
| 1.531 | 1.244 | 100.9 | 1.594 | .781 | .64 | 8807 | 3.14 | 34,600 |
| 1.515 | 1.216 | 104.3 | 1.564 | .778 | .65 | 8728 | 3.12 | 34,000 |
| 1.482 | 1.123 | 102.9 | 1.468 | .765 | .69 | 8482 | 3.00 | 32,600 |
| 1.417 | .986 | 107.3 | 1.298 | .760 | .71 | 8013 | 3.11 | 32,500 |
| | | | | | | | | Av. 32,000 |

NACA

FIG. 1

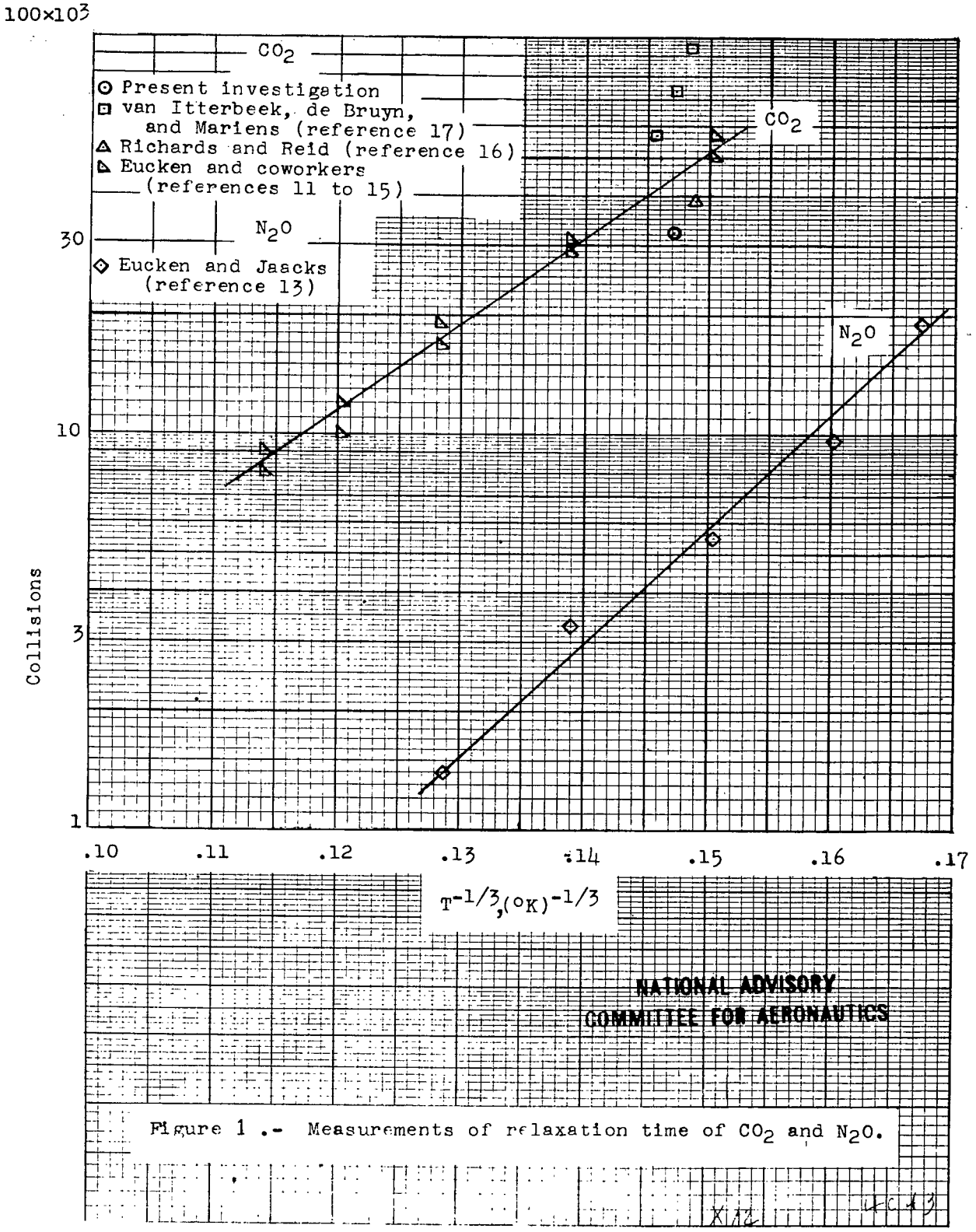


Figure 1 .- Measurements of relaxation time of $CO_2$ and $N_2O$.

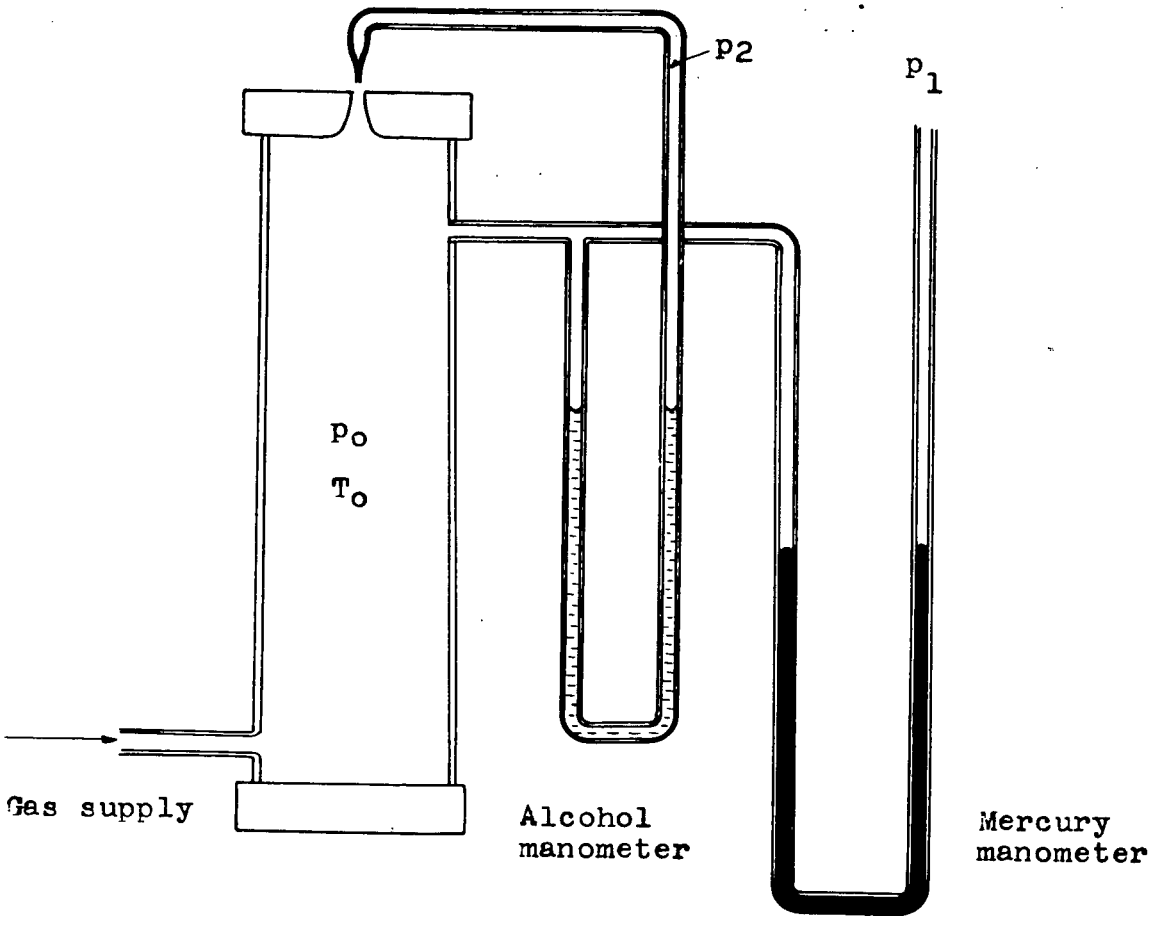


Figure 2 .- Schematized experimental arrangement.

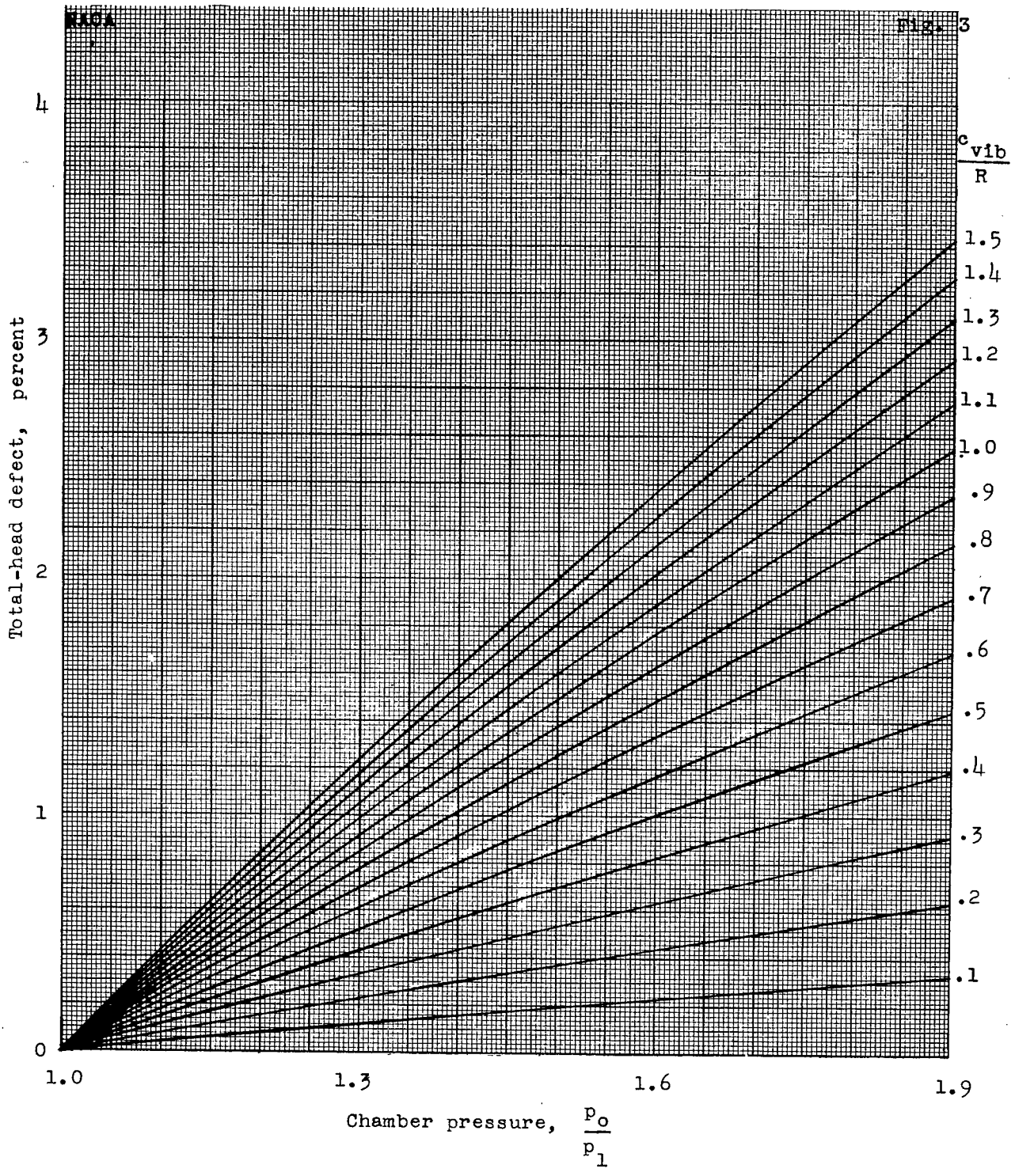


Figure 3.- Theoretical total-head defect in percent of dynamic pressure $\frac{p_o}{p_1} - 1$ for an instantaneous compression. (Linear molecules, $c_p' = 3.5R$).

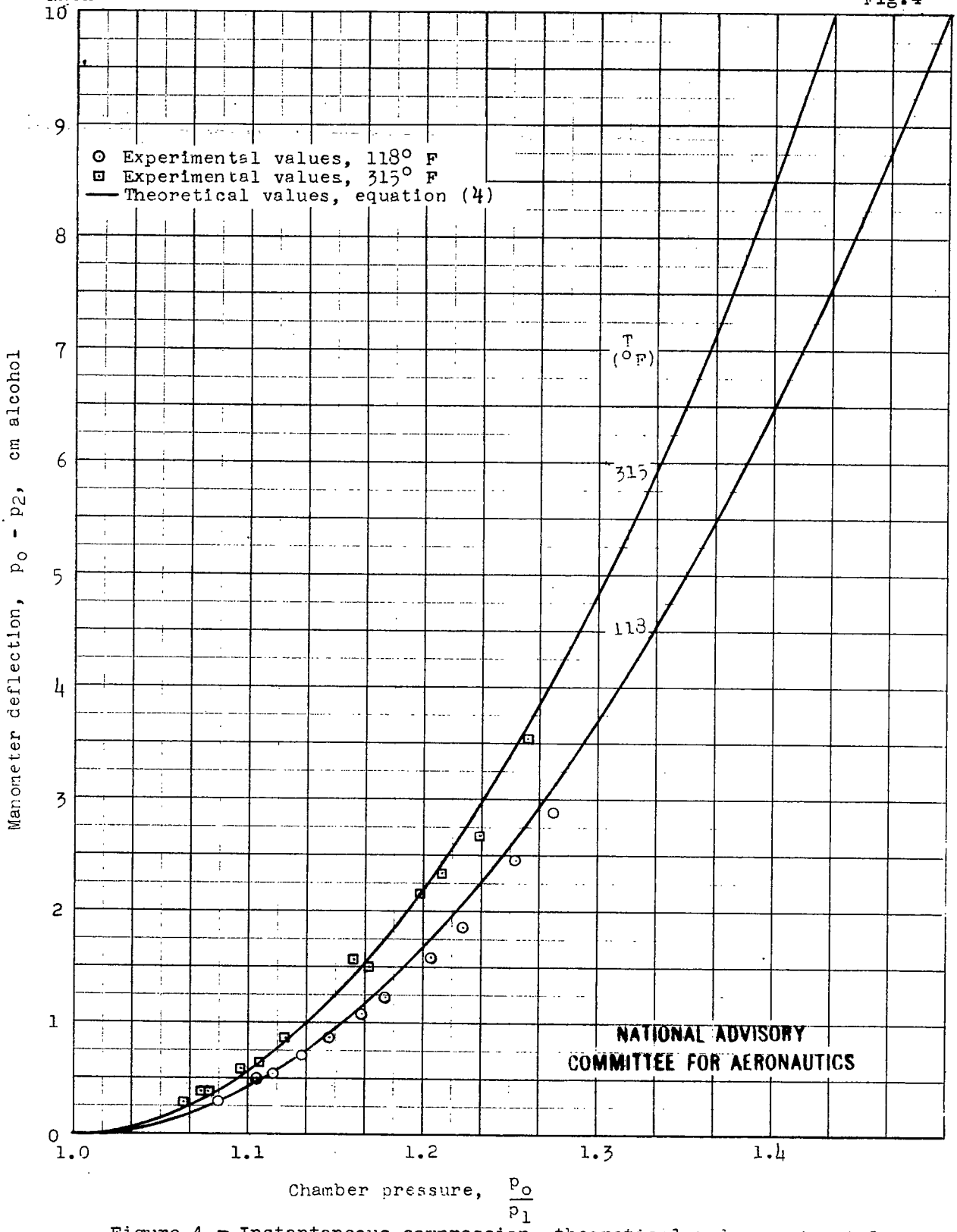


Figure 4.- Instantaneous compression, theoretical and experimental.

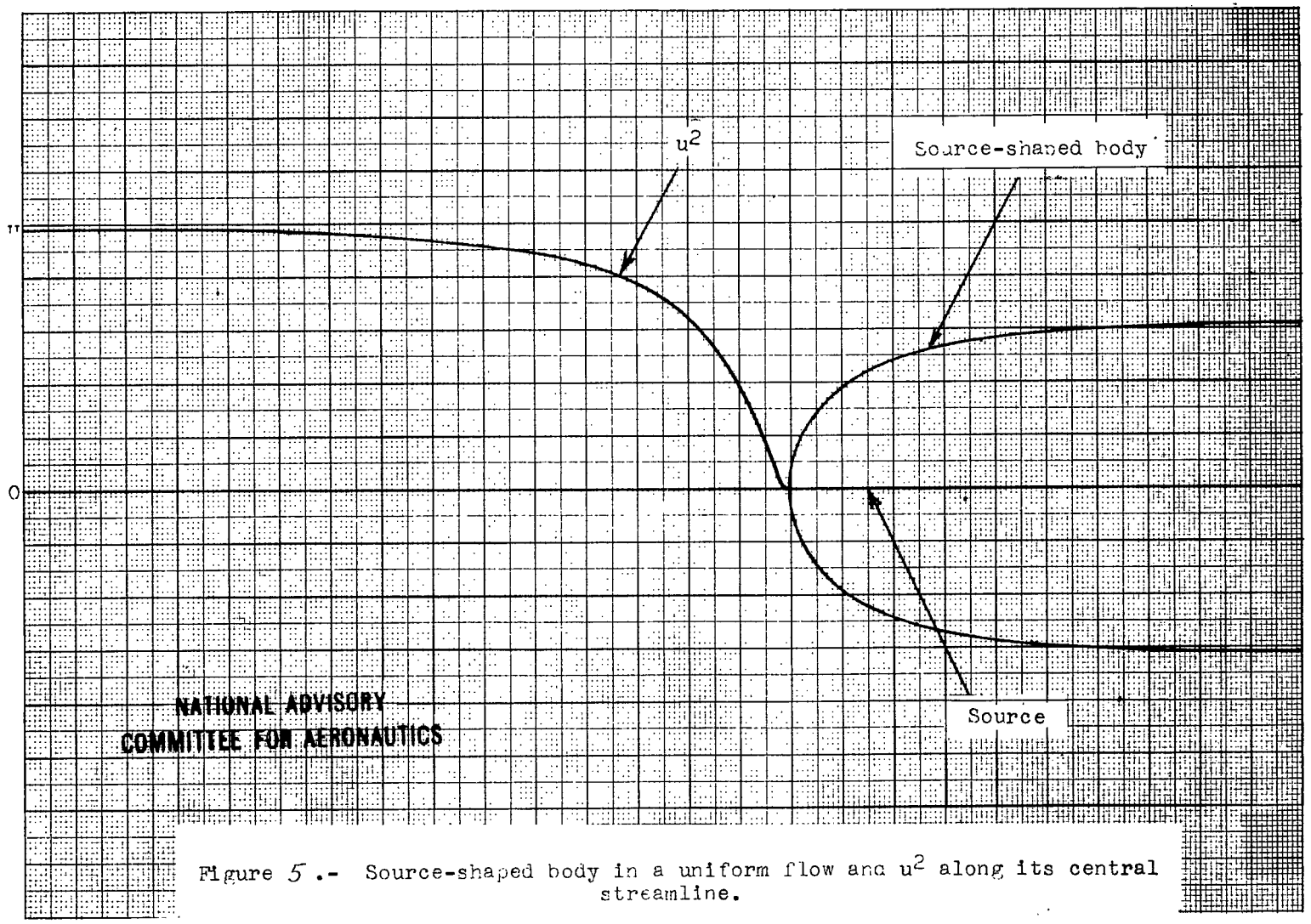


Figure 5.- Source-shaped body in a uniform flow and $u^2$ along its central streamline.

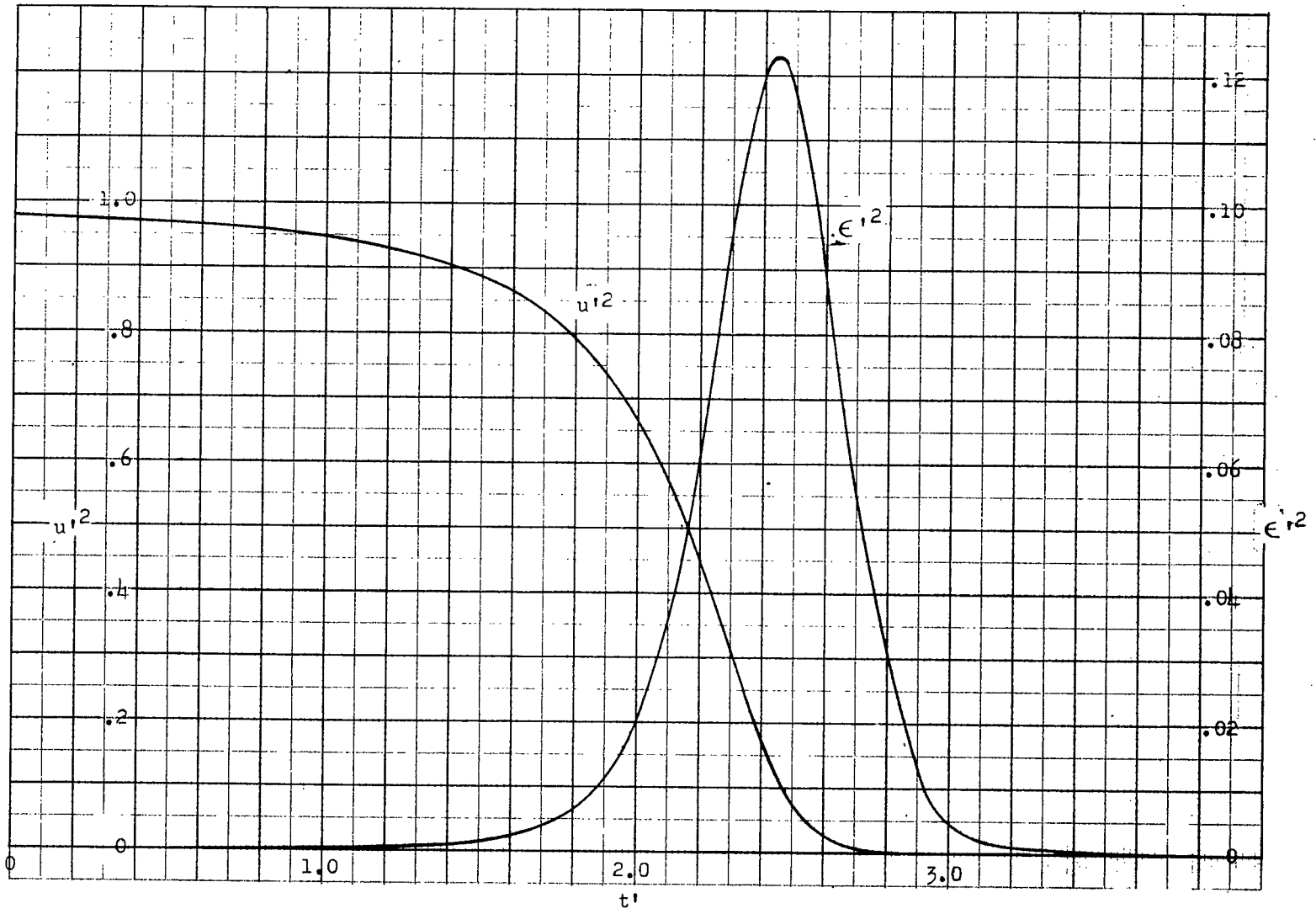


Figure 6.- Flow about a source-shaped impact tube. $u'^2$ obtained from equation (24) and $\epsilon'^2$ obtained from equation (22) for K = 3 by integration by Simpson's rule.

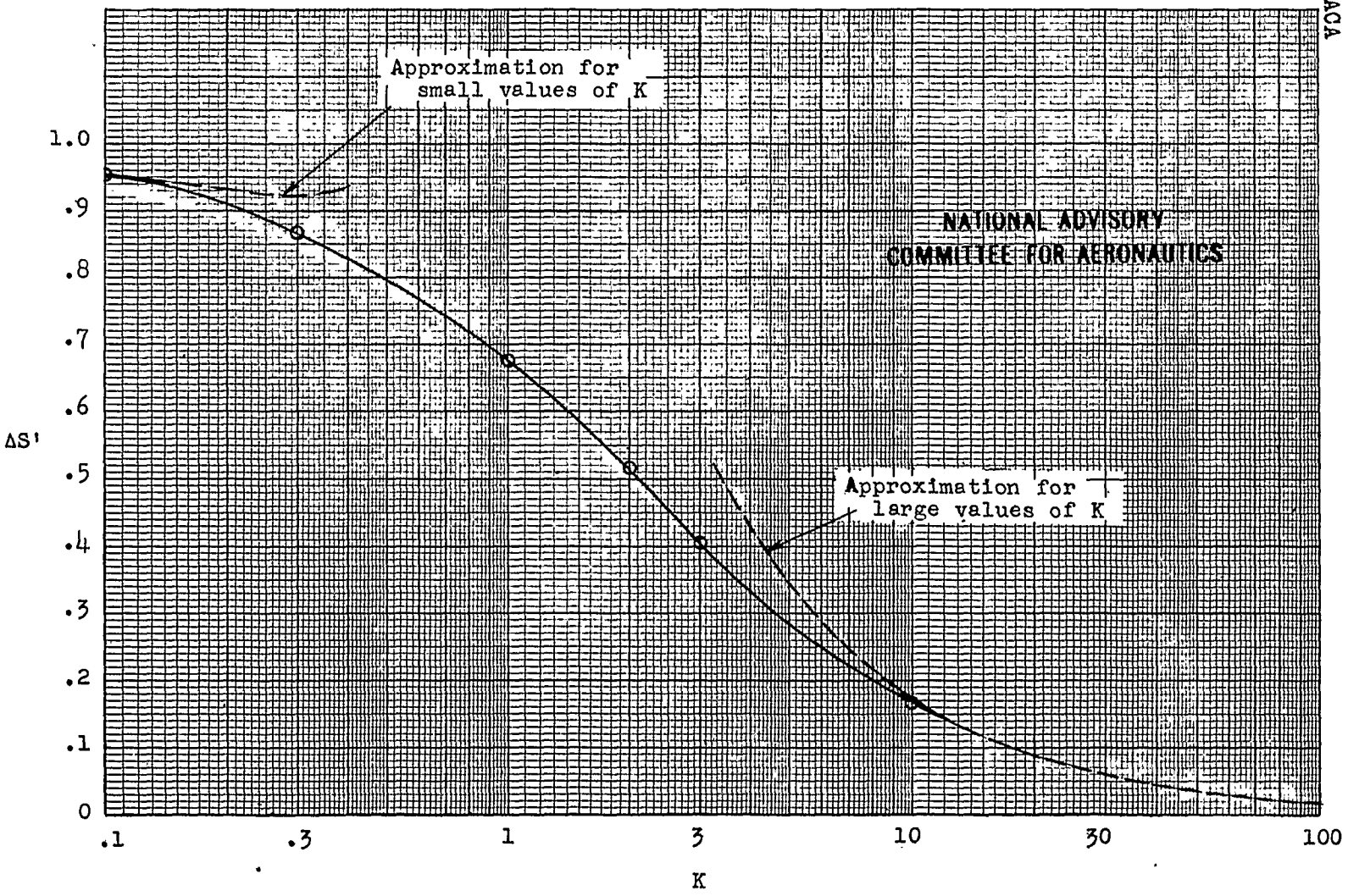


Figure 7.- The nondimensional entropy increase in the flow approaching a source-shaped impact tube. $K = d/U\tau$.

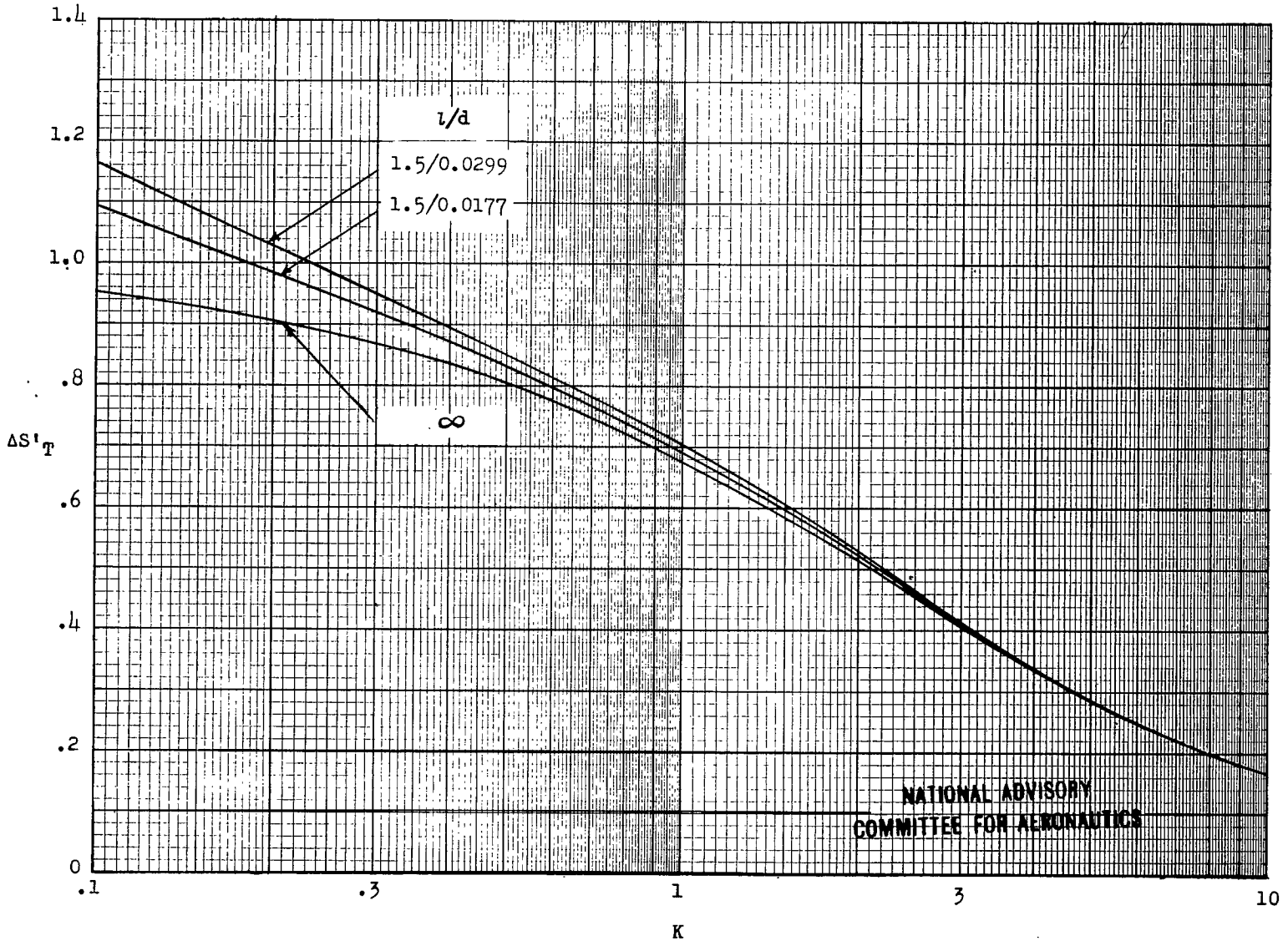


Figure 8 .- Total entropy increase in nozzle and impact tube. $\Delta S'_T = \Delta S'_{tube} + \Delta S'_N$; $K = d/U\tau$.

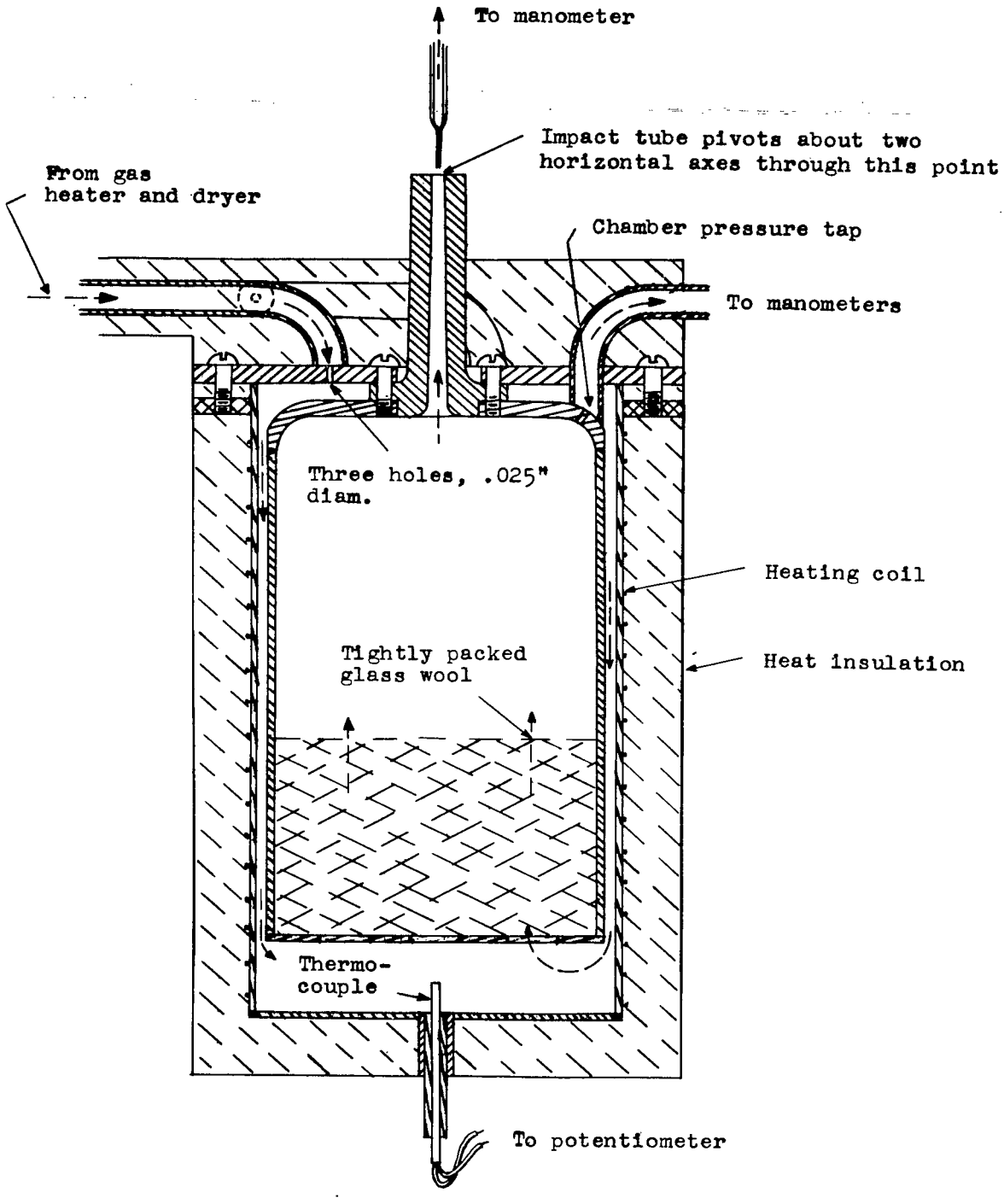


Figure 9.- Longitudinal section through chamber.

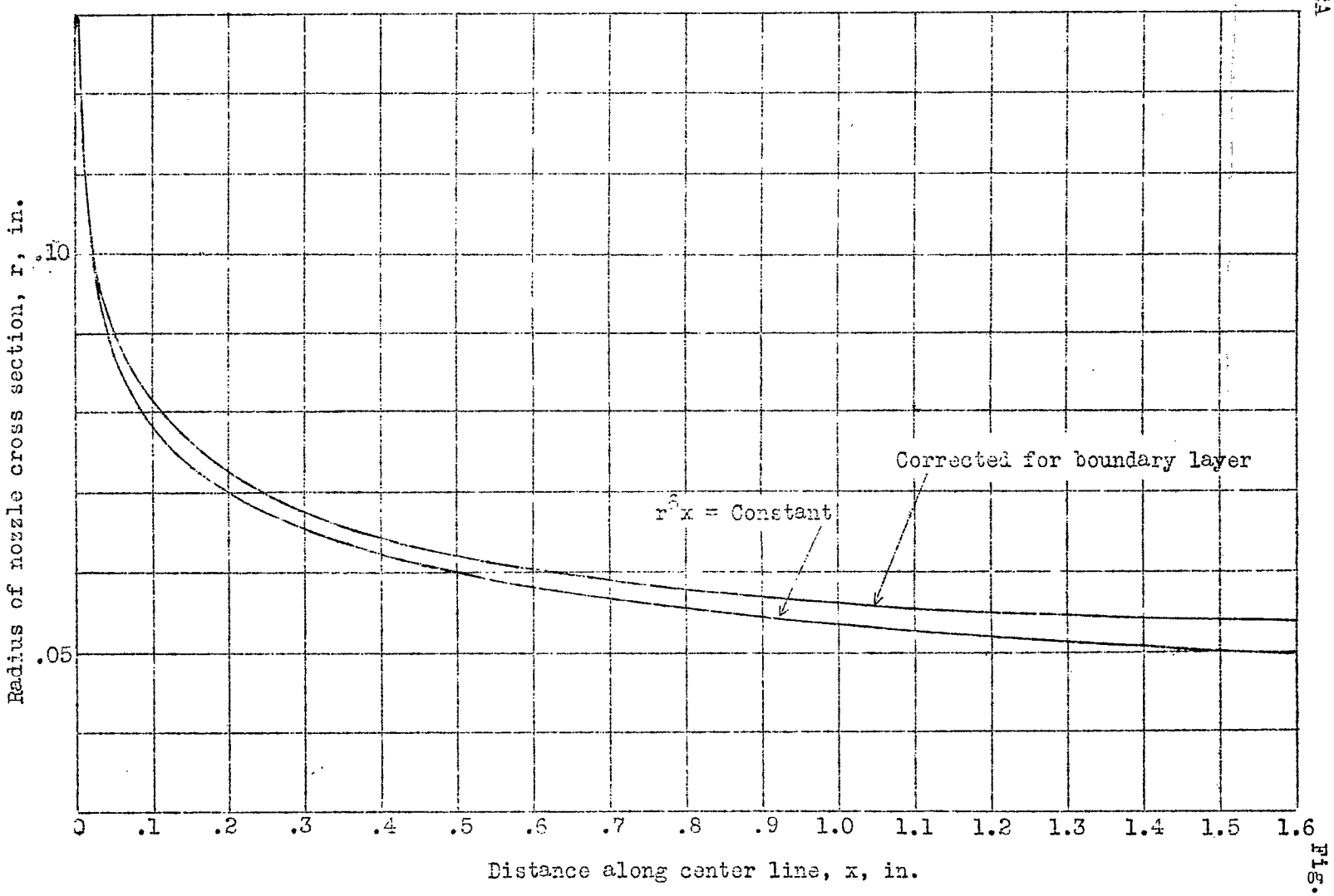




Figure 10.- Shape of nozzle, radius against distance along center line.

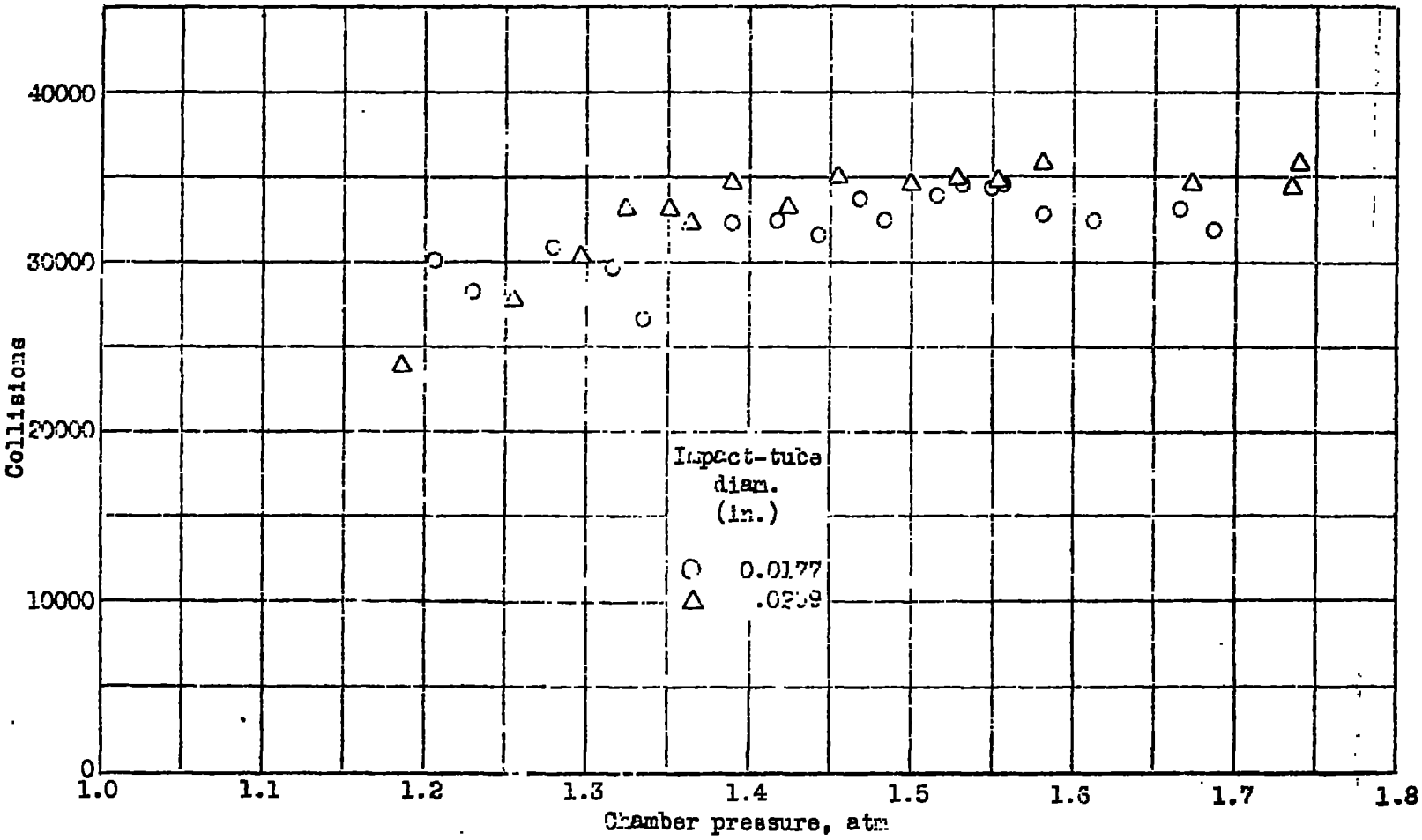


Figure 11.- Measurement of relaxation time of vibrational heat capacity in $CO_2$. Temperature near 105° F. Collisions = Relaxation time x Collisions per molecule per second.